A NOVEL 2D ANALYSIS METHOD TO CHARACTERIZE INDIVIDUAL GRAINS USING HIGH-ENERGY X-RAY MICROBEAM DIFFRACTION

E. Jimenez-Melero,[1] N. H. van Dijk,[1] L. Zhao,[2] J. Sietsma,[2] and S. van der Zwaag[3]

[1]*Fundamental Aspects of Materials and Energy, Faculty of Applied Sciences, Delft University of Technology, Mekelweg 15, 2629 JB Delft, The Netherlands*
[2]*Department of Materials Science and Engineering, Delft University of Technology, Mekelweg 2, 2628 CD Delft, The Netherlands*
[3]*Faculty of Aerospace Engineering, Delft University of Technology, Kluijverweg 1, 2629 HS Delft, The Netherlands*

ABSTRACT

The development of a novel 2D analysis method for high-energy X-ray diffraction measurements using a synchrotron microbeam is reported. Its application to study *in situ* the martensitic transformation of small individual austenite (fcc) grains embedded in a complex ferritic/bainitic/martensitic (bcc) multiphase microstructure is also reported.

INTRODUCTION

The design and development of new multiphase microstructures for specific technological applications require not only a characterization of the final microstructure, but also a detailed knowledge at the level of individual grains of the phase transformations taking place during the material processing. The availability of intense high-energy X-ray beams (50 to 300 keV) at a number of synchrotron sources has unlocked the door to unprecedented X-ray diffraction studies of a wide scope of processes in the bulk of the material [1–4]. Furthermore, the recent development of new optics components to focus the X-ray beam down to micro-dimensions [5], in combination with algebraic reconstruction techniques [6], has substantially increased the spatial resolution attainable in high-energy X-ray diffraction experiments. The state-of-the-art research in material science no longer aims at obtaining information about the average grain behavior, but at getting detailed information at the level of the ever smaller individual grains present in complex multiphase microstructures. The determination of the characteristics of individual micron-sized metastable austenite grains in the complex ferritic/bainitic/martensitic matrix of low-alloyed TRIP steels is a nice example of this trend and an example of great scientific and technological relevance [7,8].

Three-dimensional synchrotron X-ray diffraction (3DXRD) microscopy constitutes an ideal tool to study micron-sized austenite grains embedded in complex multiphase microstructures. The micro-dimensions of the high-energy X-ray beam permit to illuminate only a reduced number of grains within the bulk material, so that single diffraction spots clearly appear within the diffraction rings [1]. The integrated intensity of these diffraction spots is directly proportional to the volume of the grain from which it originates [9]. However, the diffraction spots from small grains are relatively weak and normally close to the background intensity. The existing analysis procedures consist of reducing the two-dimensional data into one dimension by binning the radial angle along a chosen diffraction ring [2,3], and then subtracting a constant background for

each diffraction spot. This significantly decreases the signal-to-noise ratio. In the present paper, a new analysis method of the two-dimensional diffraction data that takes into account the local structure of the background will be presented. This method is applied to the case of low-alloyed multiphase TRIP steels, where the martensitic transformation of metastable austenite grains contributes substantially to the outstanding combination of high strength and formability [7,10]. Because of their relatively small grain size, the study of the individual austenite grains in TRIP steels is extremely difficult with the existing 1D analysis procedures. The new method presented here substantially increases the resolution and accuracy of the characterization of individual grains.

EXPERIMENTAL

A cylindrical TRIP steel sample with a diameter of 0.5 mm with the chemical composition of 0.218 wt% C, 1.539 wt% Mn, 0.267 wt% Si, 1.750 wt% Al, 0.018 wt% P, and balance Fe was used in this study. Its complex multiphase microstructure contained micron-sized metastable austenite grains embedded in a ferritic-bainitic-martensitic matrix [4,8]. Synchrotron X-ray diffraction experiments were performed at the 3DXRD microscope available at the ID11 beam line of the European Synchrotron Radiation Facility (Grenoble, France), in order to characterize the different phases present in the TRIP microstructure at room temperature. A monochromatic X-ray microbeam with an energy of 80 keV illuminated the cylindrical sample. The grains that fulfilled the Bragg condition generated a diffraction spot on the two-dimensional detector placed behind the sample. The sample was rotated around its vertical axis over an angle of $\Delta\omega$ = 0.5° during an exposure time of 2 s. A total ω-range from -30° to +30° was covered in the experiments in subsequent exposures. Three different beam sizes were employed (17 × 17 (S), 28 × 29 (M), and 39 × 39 (L) μm^2) in order to determine whether the complete volume of the grains of interest was illuminated by the X-ray beam. The martensitic transformation of the individual austenite grains was monitored *in situ* by cooling the sample from room temperature to 100 K in steps of 20 K [10].

DATA ANALYSIS

Figure 1(a) displays a two-dimensional diffraction pattern of TRIP steel at room temperature for a selected ω-angle. The {200}, {220}, and {311} austenite reflections (fcc structure), as well as the {200}, {211}, and {220} ferrite reflections (bcc structure), have been analyzed in detail in this study. Each diffraction ring consists of a number of single spots originating from individual grains in the material, together with a powder signal stemming from diffracting grains with a size below the experimental detection limit for individual grains of 5 μm^3. The evolution of the individual grains in the microstructure can be conveniently assessed *in situ* by monitoring the position and intensity of the corresponding single diffraction spots on the detector as a function of temperature. Figure 1(b) shows a diffraction spot from the {200} austenite ring. The austenite grain from which it originated has transformed into martensite (bcc structure) during cooling, so that only the powder signal remains in the same area of the detector after cooling [see Figure 1(c)]. Such a transformation does not occur for the ferrite grains, which already have the equilibrium crystal structure.

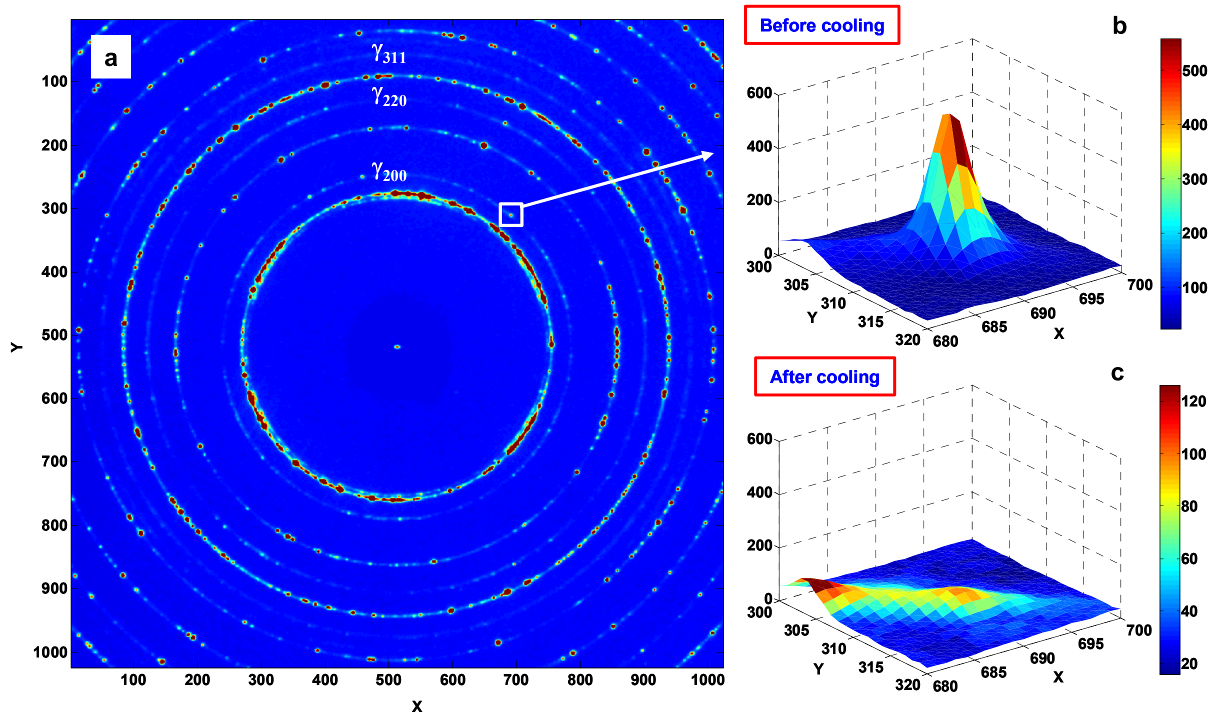

Figure 1. X-ray diffraction pattern of TRIP steel. (a) Complete two-dimensional diffraction pattern at room temperature. (b) A single austenite (γ) diffraction peak from the {200} ring at room temperature before cooling. (c) The same region as in (b) after cooling the sample to 100 K and heating back to room temperature (taken from reference [4]).

An adequate background correction is required in order to derive accurate information from the single diffraction spots. The collected intensities (I_i) can be characterized by three coordinates (X_i, Y_i, ω_i), where X_i and Y_i are the coordinates on the two-dimensional detector, while ω_i indicates the sample rotation angle. Alternatively, the polar coordinates (R_i, η_i) can be used instead of (X_i, Y_i) to specify the pixel position on the detector. They are defined as follows:

$$R_i = \left[(X_i - X_C)^2 + (Y_i - Y_C)^2\right]^{1/2} \tag{1}$$

$$\eta_i = \arctan\left[(X_i - X_C)/(Y_i - Y_C)\right] \tag{2}$$

where (X_C, Y_C) correspond to the coordinates of the beam center. Three integration boxes of increasing size can be placed symmetrically around a selected diffraction spot with a maximum intensity at (X_m, Y_m, ω_m) (see Table I). The difference between two consecutive boxes gives rise to two outer shells surrounding the inner integration box (Box 0). The characteristics of these outer shells are displayed in Table II.

We will discuss two ways in which the background correction can be applied: (1) assuming the background to be constant and (2) taking into account the local structure of the background. The simplest approach for the background correction assumes the local background to be constant.

This background contribution can be subtracted from the total intensity of the inner box (I_{Box0}^{Total}) by making use of Shell 1 or Shell 2 ($I_{corr}^{Total}(k) = I_{Box0}^{Total} - I_{BG}(k) * N_0$, with k = 1, 2). These two corrected intensities can be used to check that the background correction was performed adequately, and that the size of the integration box was optimal. Three cases can occur:

$$I_{corr}^{Total}(1) < I_{corr}^{Total}(2)\text{: not all the Bragg intensity is included in Box 0 (} I_{BG}(1) \text{ too large)} \quad (3)$$

$$I_{corr}^{Total}(1) > I_{corr}^{Total}(2)\text{: overlap with neighboring peaks (} I_{BG}(2) \text{ too large)} \quad (4)$$

$$I_{corr}^{Total}(1) \cong I_{corr}^{Total}(2)\text{: the size of Box 0 is optimal (} I_{BG}(1) \approx I_{BG}(2)\text{)} \quad (5)$$

When the condition in Eq. (5) occurs, the resultant intensity can be translated into the corresponding grain volume [9]. Furthermore, the analysis of the same region at the detector and in ω-range for the three beam sizes allows for the determination if the studied grain was completely illuminated by the X-ray beam.

Table I. Description of the three integration boxes.

	Number of pixels	Total intensity
Box 0	$N_0 = \Delta X_0\, \Delta Y_0\, \Delta\omega_0$	$I_{Box0}^{Total} = \sum_{i=1}^{N_0} I_i$
Box 1	$N_1 = (\Delta X_0 + 2)(\Delta Y_0 + 2)(\Delta\omega_0 + 2)$	$I_{Box1}^{Total} = \sum_{i=1}^{N_1} I_i$
Box 2	$N_2 = (\Delta X_0 + 4)(\Delta Y_0 + 4)(\Delta\omega_0 + 4)$	$I_{Box2}^{Total} = \sum_{i=1}^{N_2} I_i$

Table II. Characteristics of the two outer shells.

	Number of pixels	Average background intensity
Shell 1	$N(Shell1) = N_1 - N_0$	$I_{BG}(1) = (I_{Box1}^{Total} - I_{Box0}^{Total})/(N_1 - N_0)$
Shell 2	$N(Shell2) = N_2 - N_1$	$I_{BG}(2) = (I_{Box2}^{Total} - I_{Box1}^{Total})/(N_2 - N_1)$

The constant background correction procedure can be applied when the selected diffraction spot is much more intense than the background intensity, as in the case for ferrite diffraction spots. However, when the diffraction spot to be analyzed is relatively weak, as in the case for the retained austenite grains, the local background structure can not be neglected. The background is concentrated along the diffraction ring, because of the presence of a significant amount of small diffracting austenite grains and tails from neighboring single diffraction spots. The background contribution is then assumed to depend only on the distance to the center of the detector (R),

based on the occurrence of this relatively strong powder signal without apparent texture along the diffraction rings. In this case, a distribution of intensities as a function of the distance R can be derived for each of the two shells, so that the intensity of an element j of that distribution at a distance R_i results from an average over M pixel intensities with the same R_i value (binned in integer pixel numbers):

$$I_{BG,j}(R_i) = \frac{\sum_{i=1}^{M} I_i(R_i)}{M} \quad (6)$$

Figure 2 displays the intensity distribution for both shells, together with an equivalent distribution for Box 0, in the case of a ferrite and an austenite diffraction spot. A reliable distribution without discontinuities can only be obtained when a significant number of pixel intensities (M) is used to obtain each $I_{BG,j}(R_i)$. Typically the number of pixels involved in a single diffraction spot is of the order of three hundred pixels or higher.

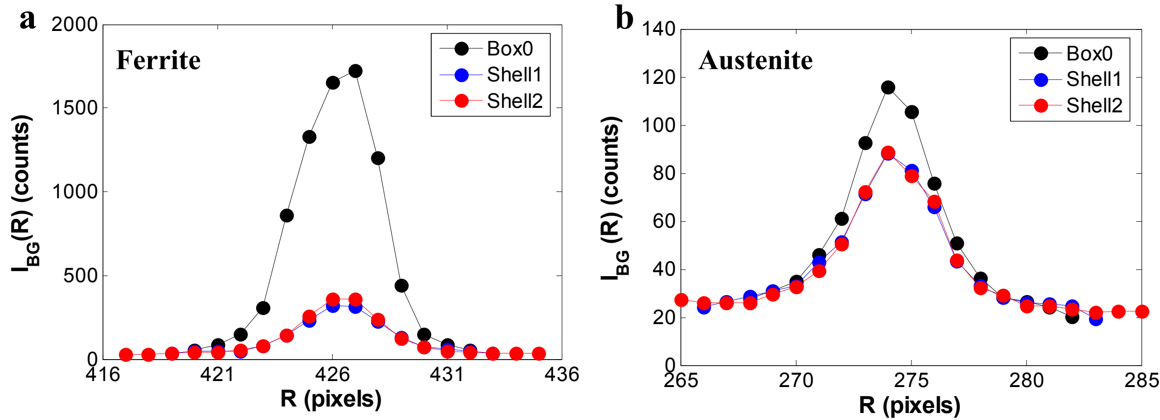

Figure 2. Distribution of intensities as a function of the distance to the center of the detector (R) for Box 0, Shell 1, and Shell 2, in the case of (a) a ferrite and (b) an austenite diffraction spot.

Once an equivalent distribution has been obtained for Shell 1 and 2, the total intensity in Box 0 can be obtained by subtracting from each pixel intensity (I_i) the $I_{BG,j}(R_i)$ with the same R_i value (rounded to an integer number), according to:

$$I_{peak} = \sum_{i=1}^{N_0} \left[I_i(X_i, Y_i, \omega_i) - I_{BG,j}(R_i) \right] = \sum_{i=1}^{N_0} \Delta I(X_i, Y_i, \omega_i) \quad (7)$$

The total intensity I_{peak} is directly proportional to the volume of the grain from which the diffraction spot originated [9]. In this way, the volume of the austenite grains can be determined at each temperature, so that its transformation into martensite can be monitored *in situ* during cooling. Figure 3 displays the volume of an individual austenite grain as a function of temperature for the two proposed background correction procedures. The subtraction of a non-constant background demonstrates that this grain was completely illuminated by the medium and large beam sizes. This grain transforms completely into martensite at a temperature of 230 K.

The corrected pixel intensities [$\Delta I(X_i,Y_i,\omega_i)$] can not only be used to determine the integrated peak intensity and hence the corresponding grain volume, but also to derive the peak position and the peak width from the weighted averages with respect to the different coordinates:

$$< z > = \sum_{i=1}^{N_0} z_i \cdot \Delta I(X_i, Y_i, \omega_i) / \sum_{i=1}^{N_0} \Delta I(X_i, Y_i, \omega_i) \tag{8}$$

$$< z^2 > = \sum_{i=1}^{N_0} z_i^2 \cdot \Delta I(X_i, Y_i, \omega_i) / \sum_{i=1}^{N_0} \Delta I(X_i, Y_i, \omega_i) \tag{9}$$

$$\sigma_z^2 = < z^2 > - < z >^2 \tag{10}$$

where $z = \omega$, R, η (or X, Y). The peak position ($<R>$) can be translated into the lattice parameter of the corresponding grain [10], which in turn contains information about the chemical content of the grain and local strains, if present. The peak widths serve to study the grain mosaicity and the spread in lattice parameter. It is worth noting that all this information can be derived from a single diffraction spot without any assumption about its shape. The error in the derived parameters can be consistently evaluated based on Poisson statistics.

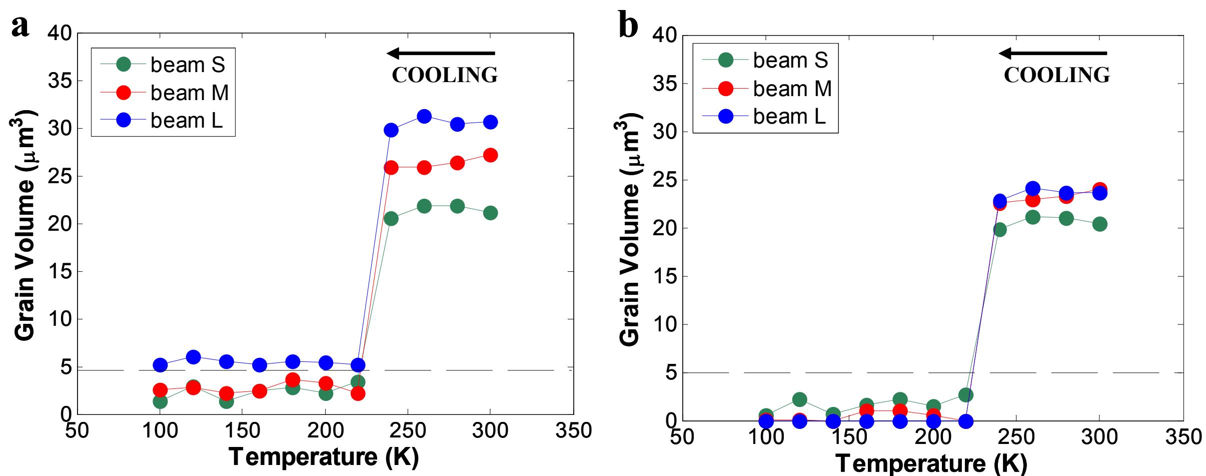

Figure 3. Temperature dependence of the volume of an individual austenite grain derived from the collected integrated intensity for the three beam sizes, using (a) constant and (b) non-constant background correction. The dashed lines indicate the detection limit for individual grains. The marker size corresponds to the experimental error.

With the developed method, the stability of individual austenite grains with respect to the martensitic transformation can be assessed as a function of their microstructural parameters such as grain size, chemical composition, and local strains. This novel analysis method can also be applied for a fast evaluation of a large number of grains simultaneously. Since this method allows the automated analysis of relatively small grains close to the detection limit, new insights into the first stages of the formation of new grains within the bulk of multiphase microstructures are envisaged.

REFERENCES

[1] Poulsen, H. F. *Three-Dimensional X-ray Diffraction Microscopy: Mapping Polycrystals and their Dynamics*; Springer: Berlin, 2004.

[2] Lauridsen, E. M.; Juul Jensen, D.; Poulsen, H. F.; Lienert, U. *Scr. Mater.* **2000**, *43*, 561–566.

[3] Offerman, S. E.; van Dijk, N. H.; Sietsma, J.; Grigull, S.; Lauridsen, E. M.; Margulies, L.; Poulsen, H. F.; Rekveldt, M. Th.; van der Zwaag, S. *Science* **2002**, *298*, 1003–1005.

[4] Jimenez-Melero, E.; van Dijk, N. H.; Zhao, L.; Sietsma, J.; Offerman, S. E.; Wright, J. P.; van der Zwaag, S. *Scr. Mater.* **2007**, *56*, 421–424.

[5] Lienert, U.; Schulze, C.; Honkimäki, V.; Tschentscher, Th.; Garbe, S.; Hignette, O.; Horsewell, A.; Lingham, M.; Poulsen, H. F.; Thomsen, N. B.; Ziegler, E. *J. Synchrotron Radiat.* **1998**, *5*, 226–231.

[6] Poulsen, H. F.; Fu, X. *J. Appl. Crystallogr.* **2003**, *36*, 1062–1068.

[7] Militzer, M. *Science* **2002**, *298*, 975–976.

[8] Zaefferer, S.; Ohlert, J.; Bleck, W. *Acta Mater.* **2004**, *52*, 2765–2778.

[9] Warren, B. E. *X-ray Diffraction*; Dover: New York, 1990.

[10] van Dijk, N. H.; Butt, A. M.; Zhao, L.; Sietsma, J.; Offerman, S. E.; Wright, J. P.; van der Zwaag, S. *Acta Mater.* **2005**, *53*, 5439–5447.